Optimal steering controller based on backstepping technique for an underwater remotely operated vehicle (ROV)

AICHA SEDINI[1], IBRAHIM AYAD[1], ABDELLAH MOKHTARI[1] ,
BUBEKEUR DAACHI[2], LARBI BOUBCHIR[2]
[1]Aero-hydrodynamic Naval Laboratory (LAHN),
The University of Science and Technology Oran (USTO-MB), ALGERIA
[2]LIASD Laboratory, The University of Paris 8, FRANCE

Abstract: The design of Remotely Operated Vehicle (ROV) steering poses challenges due to the dynamic properties of the vessel, which vary significantly based on hydrodynamic coefficients. This paper develops a robust controller based on optimal nonlinear control combined with the backstepping technique for ROV steering in the presence of unknown bounded environmental disturbances induced by waves and ocean currents. Control performance can be guaranteed through an appropriate selection of design parameters. Results obtained for a 1-meter long ROV validate the effectiveness of the proposed controller in achieving precise position and steering control under dynamic underwater conditions.

Keyword: ROVs, Optimal control, Backstepping, Underwater Robotics, Hydrodynamic Coefficients

Received: April 29, 2024. Revised: March 21, 2025. Accepted: April 19, 2025. Published: June 2, 2025.

1. Introduction

The main challenge in the field of naval architecture is to design a Remotely Operated Vehicle (ROV) that can be controlled directly by humans through remote control from the surface, enabling access to go places where humans cannot go or where it is too dangerous to explore. ROVs play a vital role in various underwater missions, including ship hull inspections, recovering objects from the ocean floor, assisting in the development of offshore oil fields [1], inspecting subsea structures and pipelines, photographing deep-sea animals, recovering torpedoes, servicing underwater oil and gas structures, and locating historic shipwrecks. They are also instrumental in subsequent repair, maintenance, and the study of marine life [2]..

Various methods are available for studying ROV motions, such as time domain and strip theory, the latter being known for its simplicity and efficiency in calculations [3]. The strip theory method, based on Lewis transformation mapping [4] , has been adapted and compared with Maxsurf results in this work. Maxsurf packages, utilizing strip theory algorithms, offer powerful three-dimensional surface modeling systems for use in naval architecture design.

Dynamic behavior variations over time, influenced by uncertainties in hydrodynamic coefficients and environmental disturbances, often complicate controller design procedures. In this context, the influence of hydrodynamic coefficients on the dynamic behavior of AUVs was analyzed under different forward speeds and standard maneuvers [5]. An experimental determination of the longitudinal and lateral hydrodynamic coefficients of a low-speed UUV was proposed by[6]. Various control schemes, including PID controllers, have been applied to heading to track different paths.[7] and [8] have derived mathematical models of underwater remotely operated vehicles with interval parametric uncertainty and utilized PID controller synthesis. The estimation of added mass coefficient and hydrodynamics damping and the stability of the ROV were performed by [9] using the PID control. [10] present a computer effective nonlinear time-domain strip theory formulation for dynamic positioning (DP) and low-speed maneuvering with the following assumptions : the fluid flow around ships is usually considered to be inviscid and irrotational, the fluid is irrotational and the motion amplitudes and velocities are small enough.

The design and implementation of guidance and control systems for ROVs have been addressed by several researchers. Model-free second-order sliding mode control, along with ocean currents as disturbances and thruster dynamics, has been elaborated by [11] . Affected by hydrodynamic forces, ROV dynamics are nonlinear, multivariable, and subject to parameter uncertainties and external disturbances. Hence, controlling the ROV requires the ability to handle nonlinearity and adaptivity toward changing parameters and environmental disturbances.

Furthermore, recent advancements in ROV control strategies have shown promising results. LQR control with pole placement adjustment has demonstrated superior system response and reduced error indices, suggesting its potential to enhance ROV performance in real-world applications [15]. Similarly, the development of a decoupled nonlinear PID (NLPID) controller for underwater vehicle trajectory tracking has shown increased robustness through the introduction of adaptive nonlinear functions [16]. Real-time experiments confirm the effectiveness of the NLPID against disturbances and uncertainties, offering promising prospects for future underwater control research.

In parallel, robust control methods for autonomous underwater vehicles (AUVs) are being explored. One approach utilizes an online optimized PID controller with a hybrid PSO algorithm, while the other employs state feedback with linear matrix inequalities [17]. Both approaches have been evaluated for controlling depth and attitude, showing that the optimized PID controller offers better robustness and superior performance compared to LMI-based state feedback.

Another significant advancement concerns the H-infinity approach for attitude control of autonomous underwater vehicles (UUVs)[18]. This method offers increased stability, particularly crucial for roll angles.

Furthermore, a control approach based on second-order sliding mode ensures precise position tracking without the need for acceleration measurements or knowledge of robot dynamics [19] .

Efforts are also underway to model AUVs more accurately, using computational fluid dynamics software to estimate key hydrodynamic parameters and developing nonlinear compensators to improve control robustness [20].

In this paper an optimal feedback controller based on backstepping techniques is developed to track predefined position trajectories. A local output feedback controller is derived by means of the differential riccati equations. This will emphasize not only the robustness performance but the choice of the adaptation matrix also [12] . Simulation results has been presented to show the effeteness of the proposed methode.

2. ROV Modeling

The three coordinate systems are introduced; the earth-fixed frame and the body-fixed frame shown in Fig-(1). The earth-fixed frame is regarded as a space-fixed inertial frame, and its origin and direction are the same as those of the body-fixed frame at initial time of maneuver. The maneuvering motion in three degrees of freedom in the horizontal plane is represented by Newton's second law:

Thrusters are usually in a balanced vector configuration to provide the most precise control possible. Without having the proper thrust, the ROV can be overwhelmed by the environmental conditions and thus unable to perform the desired tasks. Adding the hydrodynamic, hydrostatic, and propulsion forces and moments yield the total forces and moments acting on the ROV's body. These total forces and moments determine the position and orientation of the ROV. This last will maneuver through the water with five electric bilge pumps motors. The bilge pumps have been modified and refitted with propellers attached to its shaft for thrust generation, instead of impellors. to allow the pump to push water in both directions rather than just one.Two of the motors (4,5) will be used for movement in the XY-plane, with one mounted on each corner of the ROV frame. Three motors (1,2,3) will be mounted vertically making triangular form, to control movement in the Z-direction (Fig-1). The ROV will be slightly positively buoyant overall, to allow recovery in the case of a catastrophic failure underwater. The Z-plane motors will provide thrust downward or upward to keep the ROV in a spcified underwater deep during operation.To analyze the maneuvering performance, a mathematical model with optimal hydrodynamic parameters must be developed to describe precisely the motion [13] . The desired trajectory is a function of time in terms of generalized positions and their corresponding velocities and accelerations. Thus, it is of interest to develop consistent control methods that yield good performance on real systems.

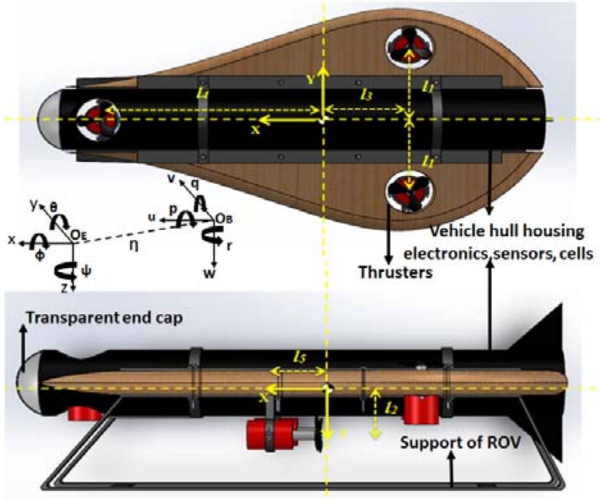

Figure 1. Design of ROV

Let the system be represented as:

$$\begin{bmatrix} \dot{\eta} = J_C(\eta_2)\nu \\ \dot{v} = M^{-1}(\dot{v})(\tau - C(\dot{v})v - D(v)v - g(\eta)) \end{bmatrix} \quad (1)$$

with $v = \begin{bmatrix} v_1 \; v_2 \end{bmatrix}^T; v_1 = \begin{bmatrix} u \; v \; w \end{bmatrix}^T; v_2 = \begin{bmatrix} p \; q \; r \end{bmatrix}^T; v_1$ and v_2 denote the linear and angular velocity vector respectively with coordinates in the body-fixed frame. τ is used to describe the forces and moments acting on the vehicle in the body-fixed frame with:

$$\tau = \begin{bmatrix} \tau_1 \\ \tau_2 \end{bmatrix} = \begin{bmatrix} L_1 \\ L_2 \end{bmatrix} U \tag{2}$$

and

$$L_1 = \begin{bmatrix} 1 & 1 & 0 & 0 & 0 \\ 0 & 0 & 0 & 0 & 0 \\ 0 & 0 & -1 & -1 & -1 \end{bmatrix};$$

$$L_2 = \begin{bmatrix} 0 & 0 & l_1 & -l_1 & 0 \\ -l_5 & -l_5 & l_3 & l_3 & -l_4 \\ l_2 & -l_2 & 0 & 0 & 0 \end{bmatrix};$$

$$U = \begin{bmatrix} T_1 \; T_2 \; T_3 \; T_4 \; T_5 \end{bmatrix}^T$$

$\eta = \begin{bmatrix} \eta_1 \; \eta_2 \end{bmatrix}^T$;with $\eta_1 = \begin{bmatrix} x \; y \; z \end{bmatrix}^T$; $\eta_2 = \begin{bmatrix} \phi \; \theta \; \psi \end{bmatrix}^T$; η_1 and η_2 denote the position and orientation vector with coordinates in the earth-fixed frame.

and

$$J_C(\eta_2) = \begin{bmatrix} J_{C1}(\eta_2) & 0_{3\times3} \\ 0_{3\times3} & J_{C2}(\eta_2) \end{bmatrix} \tag{3}$$

with $J_{C1}(\eta_2)$ and $J_{C2}(\eta_2)$ is the transformation matrix related to Euler angles

$$J_{C1}(\eta_2) = \begin{bmatrix} C\theta C\psi & S\theta S\phi C\psi - S\psi C\phi & S\theta C\phi C\psi + S\psi S\phi \\ C\theta S\psi & S\theta S\phi S\psi + C\psi C\phi & S\theta C\phi S\psi - C\psi S\phi \\ -S\theta & C\theta S\phi & C\theta C\phi \end{bmatrix} \tag{4}$$

$$J_{C2}(\eta_2) = \begin{bmatrix} 1 & S\phi T\theta & C\phi T\theta \\ 0 & C\phi & -S\phi \\ 0 & S\phi/C\theta & C\phi/C\theta \end{bmatrix}; \theta \neq \frac{\pi}{2} \pm k\pi \tag{5}$$

where $C. = \cos(.); S. = \sin(.); T. = \tan(.)$.

3. Optimal Backstepping Controller Design

Let the system be represented in hierarchical form :

$$\begin{aligned} \dot{x}_1 &= A_{13}x_3 \\ \dot{x}_2 &= A_{24}x_4 \\ \dot{x}_3 &= A_{33}x_3 + A_{34}x_4 + B_{31}u_1 + B_{32}u_2 + g_{31}w_3 \\ \dot{x}_4 &= A_{43}x_3 + A_{44}x_4 + B_{41}u_1 + B_{42}u_2 + g_{41}w_4 \end{aligned} \tag{6}$$

with $x_1 = \eta_1; x_2 = \eta_2; x_3 = \nu_1; x_4 = \nu_2$;

The controller performance was studied for laboratory prototype of the ROV with the constant parameters : $m = 13.5820Kg$; $xg = -0.087$; $yg = 0$; $zg = 0$; $xb = -0.087$; $yb = 0$; $zb = -0.027$; $Ixx = 0.2429$; $Iyy = 0.8794$; $Izz = 1.0570$; $l1 = 0.16; l2 = 0.14; l3 = 0.185; l4 = 0.35; l5 = 0.12; m = 13.5820Kg$; $xg = -0.087$; $yg = 0$; $zg = 0$; $xb = -0.087$; $yb = 0$; $zb = -0.027$; $Ixx = 0.2429$; $Iyy = 0.8794$; $Izz = 1.0570$; $l1 = 0.16; l2 = 0.14; l3 = 0.185; l4 = 0.35; l5 = 0.12$;

the matrices $A_{ij\ (3\times3)}$ are represented as follow:

$$A_{13} = J_{C1}(\eta_2); A_{24} = J_{C2}(\eta_2);$$

$$\begin{gathered} a_{33\_11} = -4.947 - 0.01q - 0.198w \\ a_{33\_12} = .872r - 0.0149p \\ a_{33\_13} = -1.025 - .852q + 0.046u \\ a_{33\_21} = -1.052r - 0.0893p - 0.573v \\ a_{33\_22} = -8.128 - 0.215q - 2.417w + 0.208u \\ a_{33\_23} = .688p - 0.335r + 1.558v \\ a_{33\_31} = -0.085 + 0.571q - 0.169w \\ a_{33\_32} = 0.0149r - 0.592p \\ a_{33\_33} = -9.343 + 0.00201q + 0.0395u \end{gathered}$$

$$\begin{gathered} a_{34\_11} = -0.022r - 0.001p + 0.0205v \\ a_{34\_12} = 0.297 + -0.0788q - 0.634w + 0.00254u \\ a_{34\_13} = -0.088r - 0.0581p + 0.389v \\ a_{34\_21} = -0.205 - 0.205q + 0.564w - 0.089u \\ a_{34\_22} = -0.254r + 0.245v + 0.025p \\ a_{34\_23} = 0.722q + 0.085u + 1.219 + 0.305w \\ a_{34\_31} = -0.077r - 0.043p - 0.254v \\ a_{34\_32} = 0.042q - 0.011w - 3.453 + 0.1u \\ a_{34\_33} = -0.002r + 0.004p - 0.01v \end{gathered}$$

$$\begin{gathered} a_{43\_11} = -3.761r - 0.32p - 2.052v \\ a_{43\_12} = -29.058 - 5.258q - 44.234w + 0.744u \\ a_{43\_13} = -1.119p - 6.126r + 28.53v \\ a_{43\_21} = 1.55 + .17q + 3.186w \\ a_{43\_22} = -0.273r + 0.232p \\ a_{43\_23} = -0.047q + 16.352 - 0.745u \\ a_{43\_31} = -2.684r - 1.073p - 6.885v \\ a_{43\_32} = -5.052 + 0.672q - 3.181w + 2.497u \\ a_{43\_33} = 0.904p - 0.441r + 2.052v \end{gathered}$$

$$a_{44\_11} = -0.735q + 2.015w - 3.757 - 0.32u$$
$$a_{44\_12} = -4.654r + 5.806v + 0.089p$$
$$a_{44\_13} = 14.215q + 3.879u + 4.356 + 5.578w$$
$$a_{44\_21} = 0.358r + 0.017p - 0.332v$$
$$a_{44\_22} = 0.008q + 0.198w - 4.816 - 0.04u$$
$$a_{44\_23} = 0.027r - 0.07p + 0.192v$$
$$a_{44\_31} = -3.377q - 0.457w - 0.270 - 1.072u$$
$$a_{44\_32} = -0.335r - 0.632v + 0.3p$$
$$a_{44\_33} = 0.95q + 0.112u - 8.293 + 0.401w$$

$$B_{31} = \begin{bmatrix} 0.064 & 0 & 0.001 \\ 0 & 0.069 & 0 \\ 0.001 & 0 & 0.044 \end{bmatrix}$$

$$B_{32} = \begin{bmatrix} 0 & -0.02 & 0 \\ 0.245 & 0 & 0.09 \\ 0 & -0.017 & 0 \end{bmatrix}$$

$$B_{41} = \begin{bmatrix} 0 & 0.245 & 0 \\ -0.02 & 0 & -0.017 \\ 0 & 0.09 & 0 \end{bmatrix}$$

$$B_{42} = \begin{bmatrix} 4.483 & 0 & 0.032 \\ 0 & 0.323 & 0 \\ 0.323 & 0 & 1.082 \end{bmatrix}$$

$$g_{31} = \begin{bmatrix} -0.075 & 0 & 0 \\ 0 & 0.913 & 0 \\ -0.064 & 0 & 0 \end{bmatrix}$$

$$g_{41} = \begin{bmatrix} 0 & 16.623 & 0 \\ 1.205 & 0 & 0 \\ 0 & 1.187 & 0 \end{bmatrix}$$

$$w_3 = w_4 = \begin{bmatrix} S\theta \\ C\theta S\phi \\ C\theta C\phi \end{bmatrix}$$

$$u_1 = \tau_1; u_2 = \tau_2$$

. Assuming that system is stabilizable, then the following theorem is established [14].

Theorem 1 *Consider the hierarchical system 6 with the assumption that pair (A_{ij}, B_{ij}) has to be stabilizable; then there exists a virtual control v_i and a positive semi-definite matrix P_i such that the subsystem can be represented in the form*

$$\dot{z}_i(t) = A_{ij}z_i(t) - A_{ij}z_{i-1}(t) - \dot{v}_{i-1}(t) \\ -B_{ij}(t)v_i(t) - g_{ij}(t)w_i$$

with the new variable z defined as

$$z_i(t) = v_{i-1}(t) - \phi_{i-1}(t)$$

and the virtual backstepping controller v :

$$B_{ij}(t)v_i(t) = B_{ij}(t)R_i^{-1}(t)B_{ij}^T(t)P_i z_i(t) + \dot{v}_{i-1}(t) \\ -A_{ij}v_{i-1}(t) - P_i^{-1}B_{ij}^T(t)P_{i-1}z_{i-1}(t)$$

which asymptotically stabilizes the disturbance free system.

Proof. Let the cost function with constrain :

$$\bar{J}(x,u,\lambda) = J(x,u) + \int_{t_1}^{t_2} \lambda(t)^T (f(x,u,t) - \dot{x})(t)dt \quad (7)$$

With

$$X \times U \ni (x,u) \to J(x,u) = \varphi(x(t_2),t_2) + \int_{t_1}^{t_2} L(x(t),u(t),t)dt \quad (8)$$

Let

$$H(x(t),u(t),\lambda(t),t) = L(x(t),u(t),t) + \lambda(t)^T f(x,u,t) \quad (9)$$

the Hamiltonian of problem 7. Note that the conditions of optimality are:

$$\begin{aligned} \dot{x} &= f(x,t) + g_1(x,t)w + g_2(x,t)u \quad (10) \\ x(t_0) &= x_0 \\ \dot{\lambda}(t)^T &= -\frac{\partial H}{\partial x}(x,u,\lambda) \\ \lambda^T(t_f) &= \frac{\partial \varphi(x(t_f),t_f)}{\partial x(t_f)} \\ \frac{\partial H}{\partial u} &= 0 \end{aligned}$$

the proof will de detailled in step(1 to 4): ■

3.1 step1

Let

$$\begin{aligned} \dot{x}_1 &= A_{13}v_1 \quad (11) \\ z_1 &= x_{1d} - x_1 \\ \dot{z}_1 &= \dot{x}_{1d} - \dot{x}_1 = \dot{x}_{1d} - A_{13}v_1 \end{aligned}$$

Let

$$\dot{z}_1 = A_1 z_1 + B_1 \xi_1 - G_{11} w_1 \quad (12)$$

with

$$A_1 = 0;\ B_1 = I; G_{11} = 0; \xi_1 = \dot{x}_{1d} - A_{13}v_1$$

taking

$$L_1=\frac{1}{2}z_1^T Q_1 z_1+\frac{1}{2}\xi_1^T R_1 \xi_1-\gamma_1^2 w_1^T w_1 \tag{13}$$

and

$$\phi_1(z_1,t)=\frac{1}{2}z_1^T P_1 z_1 \tag{14}$$

the hamiltonian for z_1 variable will be :

$$H_1=\frac{1}{2}z_1^T Q_1 z_1+\frac{1}{2}\xi_1^T R_1 \xi_1-\frac{1}{2}\gamma_1^2 w_1^T w_1+\lambda_1^T \dot{z}_1 \tag{15}$$

$$\begin{aligned} H_1 = {} & \frac{1}{2}z_1^T Q_1 z_1+\frac{1}{2}\xi_1^T R_1 \xi_1-\frac{1}{2}\gamma_1^2 w_1^T w_1 \\ & +\lambda_1^T\left(A_1 z_1+B_1\xi_1-G_{11}w_1\right) \end{aligned} \tag{16}$$

Applying the optimality conditions leads:

$$\dot{\lambda}_1=-\left(\frac{\partial H_1}{\partial z_1}\right)^T=-Q_1 z_1-A_1^T\lambda_1 \tag{17}$$

$$\lambda_1=\frac{\partial \phi_1(z_1,t)}{\partial z_1}=P_1 z_1 \tag{18}$$

control law is deduced from hamiltonian equation which reflect the H_∞ control law (optimality condition):

$$\frac{\partial H_1}{\partial \xi_1}+\frac{\partial H_1}{\partial w_1}=0 \Rightarrow R_1\xi_1+B_1^T\lambda_1-\gamma_1^2 w_1-G_{11}^T\lambda_1=0 \tag{19}$$

taking the worst case

$$w_1=-\frac{1}{\gamma^2}B_{11}^T\lambda_1=-\frac{1}{\gamma_1^2}G_{11}^T P_1 z_1 \tag{20}$$

leeds to

$$\xi_1=-R_1^{-1}B_1^T\lambda_1=-R_1^{-1}B_1^T P_1 z_1$$

differentiating 18 :

$$\dot{\lambda}_1=P_1\dot{z}_1+\dot{P}_1 z_1$$

comparing with 17 leads to:

$$P_1\dot{z}_1+\dot{P}_1 z_1=-Q_1 z_1-A_1^T\lambda_1$$

hence

$$\dot{P}_1 z_1=-P_1\left(A_1 z_1+B_1\xi_1\right)-Q_1 z_1-A_1^T\lambda_1$$

replacing with equation 12 and 20 the followng equation is obtained:

$$\begin{aligned} \dot{P}_1 z_1 = {} & -P_1\left(A_1 z_1+B_1\left(-R_1^{-1}B_1^T P_1 z_1\right)+\frac{1}{\gamma_1^2}G_{11}G_{11}^T P_1 z_1\right) \\ & -Q_1 z_1-A_1^T P_1 z_1 \end{aligned}$$

so

$$-\dot{P}_1=P_1 A_1+A_1^T P_1+P_1\left(\frac{1}{\gamma_1^2}G_{11}G_{11}^T-B_1R_1^{-1}B_1^T\right)P_1+Q_1 \tag{21}$$

for $A_1=0;\ B_1=I$ and $G_{11}=0$; the riccati equation became

$$-\dot{P}_1=-P_1R_1^{-1}P_1+Q_1 \tag{22}$$

with Q_1 a symmetric matrix,R_1 is a diagonal matrix; then the control law is calculated as:

$$\xi_1=-R_1^{-1}P_1 z_1=\dot{x}_{1d}-A_{13}v_1$$

Since $A_{13}=J_{C1}(\eta_2)$ and $J_{C1}^{-1}(\eta_2)=J_{C1}^T(\eta_2)$ then:

$$v_1=J_{C1}^T(\eta_2)\left(R_1^{-1}P_1 z_1+\dot{x}_{1d}\right) \tag{23}$$

3.2 Step2

Let

$$\begin{aligned} \dot{x}_2 &= A_{24}v_2 \\ z_2 &= x_{2d}-x_2 \\ \dot{z}_2 &= \dot{x}_{2d}-\dot{x}_2=\dot{x}_{2d}-A_{24}v_2 \end{aligned}$$

following the procedure as step1 then the virtual control is obtained:

$$v_2=J_{C2}^{-1}(\eta_2)\left(R_2^{-1}P_2 z_2+\dot{x}_{2d}\right)$$

3.3 step3

$$\dot{x}_3=A_{33}x_3+A_{34}x_4+B_{31}u_1+B_{32}u_2+G_{31}w_3$$

Let

$$\begin{aligned} z_3 &= v_1-x_3;\ z_4=v_2-x_4 \\ \dot{z}_3 &= \dot{v}_1-\dot{x}_3;\ \dot{z}_4=\dot{v}_2-\dot{x}_4 \end{aligned}$$

$$\dot{z}_3=\dot{v}_1-\left(A_{33}x_3+A_{34}x_4+B_{31}u_1+B_{32}u_2+G_{31}w_3\right) \tag{24}$$

$$\begin{aligned} \dot{z}_3 = {} & \dot{v}_1+A_{33}\left(z_3-v_1\right)+A_{34}\left(z_4-v_2\right) \\ & -\left(B_{31}u_1+B_{32}u_2\right)-G_{31}w_3 \end{aligned} \tag{25}$$

writing equation 24 as:

$$\dot{z}_3=A_3 z_3+B_3\xi_3-G_{31}w_3$$

with $B_3=I,\xi_3$ is obtained:

$$\xi_3=\dot{v}_1-A_{33}v_1+A_{34}z_4-A_{34}v_2-\left(B_{31}u_1+B_{32}u_2\right)$$

Let

$$\begin{aligned} L_3 = {} & \frac{1}{2}z_1^T Q_1 z_1+\frac{1}{2}z_3^T Q_3 z_3+\frac{1}{2}\xi_1^T R_1\xi_1 \\ & +\frac{1}{2}\xi_3^T R_3\xi_3-\frac{1}{2}\gamma_1^2 w_1^T w_1-\frac{1}{2}\gamma_3^2 w_3^T w_3 \end{aligned} \tag{26}$$

and

$$\phi_3 = \frac{1}{2}z_1^T P_1 z_1 + \frac{1}{2}z_3^T P_3 z_3 \tag{27}$$

the hamiltonian for z_3 variable will be :

$$H_3 = \frac{1}{2}z_1^T Q_1 z_1 + \frac{1}{2}z_3^T Q_3 z_3 + \frac{1}{2}\xi_1^T R_1 \xi_1 + \frac{1}{2}\xi_3^T R_3 \xi_3 - \frac{1}{2}\gamma_1^2 w_1^T w_1 - \frac{1}{2}\gamma_3^2 w_3^T w_3 + \lambda_1^T \dot{z}_1 + \lambda_3^T \dot{z}_3 \tag{28}$$

$$H_3 = \frac{1}{2}z_1^T Q_1 z_1 + \frac{1}{2}z_3^T Q_3 z_3 + \frac{1}{2}\xi_1^T R_1 \xi_1 + \frac{1}{2}\xi_3^T R_3 \xi_3 - \frac{1}{2}\gamma_1^2 w_1^T w_1 - \frac{1}{2}\gamma_3^2 w_3^T w_3 + \lambda_1^T \xi_1 + \lambda_3^T (A_3 z_3 + B_3 \xi_3 - G_{31} w_3)$$

Applying the optimality conditions leads:

$$\dot{\lambda}_1 + \dot{\lambda}_3 = -\left(\frac{\partial H_3}{\partial z_1}\right)^T - \left(\frac{\partial H_3}{\partial z_3}\right)^T = -Q_1 z_1 - Q_3 z_3 - A_3^T \lambda_3 \tag{29}$$

$$\lambda_1 + \lambda_3 = \frac{\partial \phi_3}{\partial z_1} + \frac{\partial \phi_3}{\partial z_3} = P_1 z_1 + P_3 z_3 \tag{30}$$

control law is deduced from hamiltonian equation (optimality condition):

$$\frac{\partial H_3}{\partial \xi_1} + \frac{\partial H_3}{\partial \xi_3} + \frac{\partial H_3}{\partial w_1} + \frac{\partial H_3}{\partial w_3} = 0$$

Sce $\frac{\partial H_3}{\partial \xi_3} + \frac{\partial H_3}{\partial w_3} = \frac{\partial H_1}{\partial \xi_1} + \frac{\partial H_1}{\partial w_1} = 0$ then

$$\frac{\partial H_3}{\partial \xi_3} + \frac{\partial H_3}{\partial w_3} = 0 \Rightarrow R_3 \xi_3 + B_3^T \lambda_3 - \gamma_3^2 w_3 - G_{31}^T \lambda_3 = 0$$

taking the worst case for perturbation

$$w_3 = -\frac{1}{\gamma_3^2} G_{31}^T \lambda_3 = -\frac{1}{\gamma_3^2} G_{31}^T P_3 z_3$$

will give

$$\xi_3 = -R_3^{-1} B_3^T P_3 z_3$$

from 30

$$\dot{\lambda}_1 + \dot{\lambda}_3 = P_1 \dot{z}_1 + P_3 \dot{z}_3 + \dot{P}_1 z_1 + \dot{P}_3 z_3 \tag{31}$$

equalizing 29 and 31 gives:

$$P_1 \dot{z}_1 + P_3 \dot{z}_3 + \dot{P}_1 z_1 + \dot{P}_3 z_3 = -Q_1 z_1 - Q_3 z_3 - A_3^T \lambda_3$$

$$\dot{P}_3 z_3 = -P_3 (A_3 z_3 + B_3 \xi_3 - G_{31} w_3) - \dot{P}_1 z_1 - P_1 \xi_1 - Q_1 z_1 - Q_3 z_3 - A_3^T P_3 z_3$$

$$\dot{P}_3 z_3 = -P_3 (A_3 z_3 + B_3 - R_3^{-1} B_3^T P_3 z_3) + \frac{1}{\gamma_3^2} G_{31} G_{31}^T P_3 z_3$$

$$\dot{P}_3 z_3 = -(P_3 A_3 + A_3^T P_3 - P_3 B_3 R_3^{-1} B_3^T P_3 + \frac{1}{\gamma_3^2} P_3 G_{31} G_{31}^T P_3 + Q_3) z_3 + \left(-\dot{P}_1 + P_1 R_1^{-1} P_1 - Q_1\right) z_1$$

taking into account 22 ,P_3 matrix is computed through the riccati equation written as:

$$-\dot{P}_3 = P_3 A_3 + A_3^T P_3 + P_3 \left(\frac{1}{\gamma_3^2} G_{31} G_{31}^T - B_3 R_3^{-1} B_3^T\right) P_3 + Q_3 \tag{32}$$

Q_3 is chosen to be a symmetric matrix. So the control is:

$$\xi_3 = \dot{v}_1 - A_{33} v_1 + A_{34} z_4 - A_{34} v_2 - (B_{31} u_1 + B_{32} u_2) = -R_3^{-1} B_3^T P_3 z_3$$

Let

$$U_1 = (B_{31} u_1 + B_{32} u_2)$$

So

$$U_1 = \dot{v}_1 - A_{33} v_1 + A_{34} z_4 - A_{34} v_2 + R_3^{-1} B_3^T P_3 z_3$$

3.4 step4

$$\dot{x}_4 = A_{43} x_3 + A_{44} x_4 + B_{41} u_1 + B_{42} u_2 + G_{41} w_4$$

following the procedure as step3 then the virtual control is obtained:

$$U_2 = \dot{v}_2 - A_{44} v_2 + A_{43} z_3 - A_{43} v_1 + R_4^{-1} B_4^T P_4 z_4 \tag{33}$$

Finally

$$\begin{bmatrix} U_1 \\ U_2 \end{bmatrix} = \begin{bmatrix} B_{31} & B_{32} \\ B_{41} & B_{42} \end{bmatrix} \begin{bmatrix} u_1 \\ u_2 \end{bmatrix}$$

Hence

$$\begin{bmatrix} u_1 \\ u_2 \end{bmatrix} = \begin{bmatrix} B_{31} & B_{32} \\ B_{41} & B_{42} \end{bmatrix}^{-1} \begin{bmatrix} U_1 \\ U_2 \end{bmatrix} \tag{34}$$

4. Simulation and Results

The controller performance was studied for laboratory prototype of the ROV with the constant parameters : $m = 13.5820Kg$; $xg = -0.087$; $yg = 0$; $zg = 0$; $xb = -0.087$; $yb = 0$; $zb = -0.027$; $Ixx = 0.2429$; $Iyy = 0.8794$; $Izz = 1.0570$;

$l1 = 0.16; l2 = 0.14; l3 = 0.185; l4 = 0.35; l5 = 0.12$; the ROV was required to move to $x = 1m : z = 1m$; $\psi = \frac{\pi}{4} rad$. An external perturbation of $0.1m$ which reflect sea wave has been introduced in the three directions: $x_p = 0.1U(t-25)$; $y_p = 0.1U(t-30)$; $\psi_p = 0.1U(t-35)$. $U(t)$ is the unit step. The desired and measured mouvements and their tracking errors are represented in figures(2, 3 ,4).The attitude angles ϕ and θ are represented in figure(5). The control inputs represented by forces are represented in figure (6). It is concluded from these figures that H_∞ controller that the choice of the pertubation vector w does not affect the performance of the controller and the technique proposed is able to catch up and follow the desired trajectory even with external perturbation.

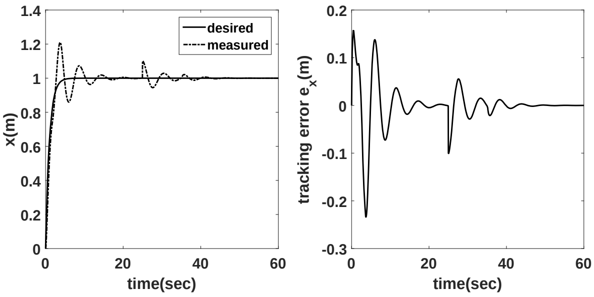

Figure 2. surge controlled output

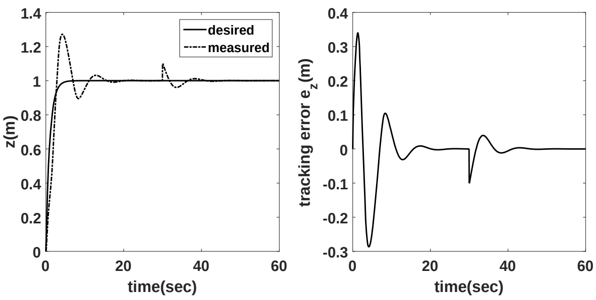

Figure 3. heave controlled output

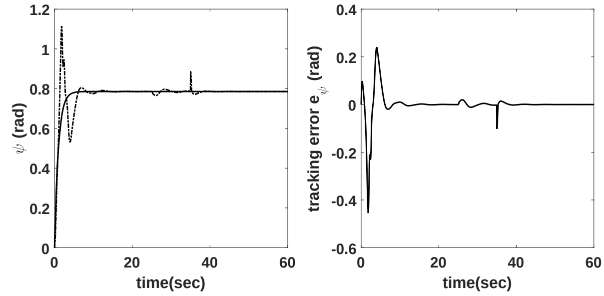

Figure 4. yaw controlled output

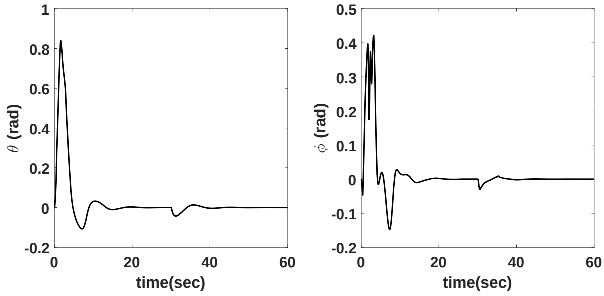

Figure 5. ϕ and θ angles

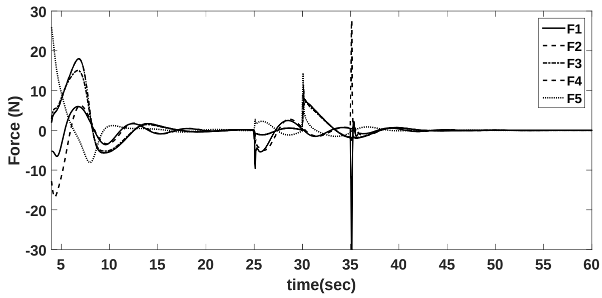

Figure 6. input forces (N)

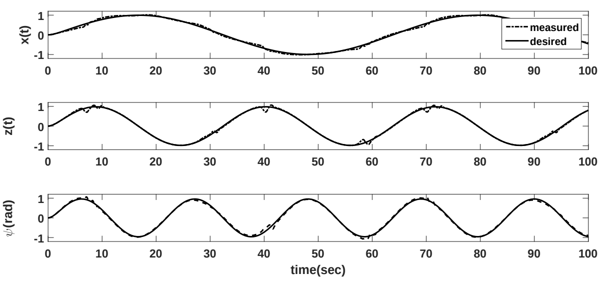

Figure 7. Sine trajectory

5. Conclusions

An optimal controller based on backstepping technique for un derwater remotely operated system has been proposed to track predefined position trajectories. The paper addresses the development of a nonlinear optimal controller which can reject from the nominal model the effect of pertur bations. Even though the mathematical model was highly nonlinear and the environmental disturbances are always presents; the proposed model representation which look linear in its parameters vector has made the hierarchical methodology of the combined controller easier to achieve. It is shown that the all over system is able to track the predefined trajectory with a truncation in the model and an environmental chosen perturbation of $0.1m$ in amplitude.

Further investigation will focus on solving algebraic state dependent riccati equation to reach global stability. The problem of state observer will be considered. A validation with real time experiments with the ROV prototype will be set to demonstrate the applicability of the considered control strategy.

The authors are grateful to the support of the ministry of higher education and scientific research in Algeria.

References

[1]. Hudson, I.R., Jones, D.O.B. and Wigham, B.D., “A review of the uses of work-class ROVs for the benefits of science: lessons learned from the SERPENT project”, Underwater Technology, 2005.

[2]. Inoue, T., Osawa, H., Yoshida, H., Tahara, J., Ishibashi, S., Ito, K., Watanabe, Y., Sawa, T. and Hyakudome T., “Sea Trial Results of ROV ABISMO for Deep Sea Inspection and Sampling”, ASME, 2008 27th International Conference on Offshore Mechanics and Arctic Engineering (OMAE2008), 2008.

[3]. Milgram, J.H. Strip theory for underwater vehicles in water of finite depth. J Eng Math 58, 31—50 (2007) doi:10.1007/s10665-006-9101-y

[4]. Do Thanh Sen, Tran Canh Vinh, "Determination of Added Mass and Inertia Moment of Marine Ships Moving in 6 Degrees of Freedom", International Journal of Transportation Engineering and Technology 2016; 2(1): 8-14, doi: 10.11648/j.ijtet.20160201.12

[5]. Mahnaz Abolvafaie, Hamid Reza Koofigar and Maryam Malekzadeh, "Classification of hydrodynamic coefficients of autonomous underwater vehicles based on sensitivity analyses in standard maneuvers", Journal of Marine Science and Technology, Vol. 26, No. 1, pp. 1-10 (2018); DOI: 10.6119/JMST.2018.02_(1).0001

[6]. Andrew Ross, Thor I. Fossen and Tor Arne Johansen, " Identification of underwater vehicle hydrodynamic coefficients using free decay tests", IFAC Proceedings Volumes, Volume 37, Issue 10, July 2004, Pages 363-368

[7]. Sergey A. Gayvoronskiy, Ivan V. Khozhaev, and Tatiana A. Ezangina ,"Motion Control System for a Remotely Operated Vehicle with Interval Parameters", International Journal of Mechanical Engineering and Robotics Research Vol. 6, No. 5, September 2017.

[8]. Budiyono, Agus & Anam, Hujjatul & Setiawan, Joga. (2015). Simulation and Dynamic Analysis of Remotely Operated Vehicle (ROV) Using PID Controller for Pitch Movement. Marine and Underwater Science and Technology. Marine and Underwater Science and Technology. 1. 23-31.

[9]. Hujjatul Anam,Joga Dharma Setiawan, and Agus Budiyono,"Simulation and Dynamic Analysis of Remotely Operated Vehicle (ROV) Using PID Controller for Pitch Movement", Marine and Underwater Science and Technology, Vol. 1, No. 1,2015.

[10]. THOR I. FOSSEN and YVIND N. SMOGELI, " Nonlinear Time-Domain Strip Theory Formulation for Low-Speed Maneuvering and Station-Keeping", modeling, identification and control,2004, Vol. 25, N. 4, pp 201—221.

[11]. Luis Govinda García-Valdovinos, Tomás Salgado- Jiménez, Manuel Bandala-Sánchez, Luciano Nava- Balanzar, Rodrigo Hernández-Alvarado and José Antonio Cruz-Ledesma, "Modelling, Design and Robust Control of a Remotely Operated Underwater Vehicle", Int J Adv Robot Syst, 2014, 11:1 | doi: 10.5772/56810.

[12]. L.T. Aguilara, Y. Orlov, L. Acho, "Nonlinear □∞control of nonsmooth time-varying systems with application to friction mechanical manipulators", Automatica 39 (2003) 1531 — 1542

[13]. Hyeon Kyu, Yoon, “Identification of hydrodynamic coefficients in ship maneuvering equations of motion by Estimation-Before-Modeling technique”, Ocean Engineering, Volume 30, Issue 18, December 2003, Pages 2379—2404.

[14]. Kaddouri Djamel, Mokhtari Abdellah and Abdelaziz Benallegue, "Attitude Optimal Backstepping Controller Based Quaternion for a UAV",Hindawi Publishing Corporation, Mathematical Problems in Engineering, Volume 2016, Article ID 8573235, 11 pages,.doi.org/10.1155/2016/8573235.

[15]. Aldana Afanador, Andres Felipe and Esteban Villegas, Helio Sneyder and Roa Prada, Sebastian," ASME International Mechanical Engineering Congress and Exposition", 2017, IMECE2017-71170, tampa florida, USA.

[16]. GUERRERO, Jesus, TORRES, Jorge, CREUZE, Vincent, et al. Saturation based nonlinear PID control for underwater vehicles: Design, stability analysis and experiments. Mechatronics, 2019, vol. 61, p. 96-105.

[17]. BEJARBANEH, Elham Yazdani, MASOUMNEZHAD, Mojtaba, ARMAGHANI, Danial Jahed, et al. Design of robust control based on linear matrix inequality and a novel hybrid PSO search technique for autonomous underwater vehicle. Applied Ocean Research, 2020, vol. 101, p. 102231.

[18]. GAVRILINA, E. A. et CHESTNOV, V. N. Synthesis of an attitude control system for unmanned underwater vehicle using H-infinity approach. IFACPapersOnLine, 2020, vol. 53, no 2, p. 14642-14649.

[19]. GARCÍA-VALDOVINOS, Luis Govinda, SALGADO-JIMÉNEZ, Tomás, BANDALASÁNCHEZ, Manuel, et al. Modelling, design and robust control of a remotely operated underwater vehicle. International Journal of Advanced Robotic Systems, 2014, vol. 11, no 1, p. 1

[20]. YANG, Rui, CLEMENT, Benoit, MANSOUR, Ali, et al. Modeling of a complex-shaped underwater vehicle for robust control scheme. Journal of Intelligent & Robotic Systems, 2015, vol. 80, p. 491-506.